Pflügers Arch – Eur J Physiol (1997) 433:390–396

ORIGINAL ARTICLE

Jiqing Guo · Tamotsu Mitsuiye · Akinori Noma

The sustained inward current in sino-atrial node cells of guinea-pig heart

Received: 22 July 1996 / Received after revision: 30 September 1996 / Accepted: 9 October 1996

Abstract Single myocytes were dissociated from the sino-atrial (SA) node of guinea-pig hearts. Only a quite small fraction of the cell population showed spontaneous action potentials and these cells were characterized by the presence of the hyperpolarization-activated cation current I_f , the delayed rectifier K^+ current I_K and the L-type Ca^{2+} current $I_{Ca,L}$ as well as by the absence of both the transient outward current I_{to} and the inward rectifier K^+ current $I_{K,1}$. After blocking I_f and I_K, depolarizing pulses from –80 mV revealed a large nicardipine-sensitive late current (NSLC). The NSLC was scarcely affected by decreasing extracellular $[Ca^{2+}]$ ($[Ca^{2+}]_o$) from 1.8 to 0.1 mM, while it was decreased significantly by depleting $[Na^+]_o$, differently from $I_{Ca,L}$. NSLC was blocked by nicardipine and was increased by Bay K 8644. NSLC was increased by isoprenaline and the additional application of acetylcholine reversed the increase of this current. We conclude that NSLC is largely composed of I_{st} described in the rabbit SA node pacemaker cells, and that I_{st} is unique for the pacemaker cells in mammalian SA node cells. Most of the quiescent cells showed neither I_f nor I_{st}.

Key words Cardiac pacemaker cell · Sinoatrial node cell · Spontaneous action potential · Sustained inward current · Guinea-pig

Introduction

Recently, a novel inward current was found in spontaneously active sino-atrial (SA) node cells of the rabbit heart [8]. In contrast to the transient activation of the low-($I_{Ca,T}$) and high-($I_{Ca,L}$) threshold Ca^{2+} currents, the new current (the sustained inward current, I_{st}) showed little inactivation during depolarization to the pacemaker potential range. Pharmacological characteristics of I_{st} are similar to those of $I_{Ca,L}$ channels, but I_{st} is selectively carried by Na^+ [8, 9] and is activated by depolarization with a threshold between –70 and –60 mV. The SA node cells showing I_{st} also possessed the hyperpolarization-activated cation current (I_f). Both I_{st} and I_f were absent in typical atrial-type cells dissociated from the SA node. Because of these characteristics, it is suggested that I_{st} may play an important role in driving the pacemaker depolarization.

To show that I_{st} plays a principal role, it is essential to demonstrate the presence of I_{st} in a variety of species. However, because of difficulties in isolating SA node cells, voltage-clamp experiments have been carried out almost exclusively in the rabbit SA node cell. In 1992, Anumonwo et al. first succeeded in isolating SA node cells from the guinea-pig heart, but these authors studied only the delayed rectifier K^+ current (I_K) [1]. Interestingly, I_K in guinea-pig SA node cells was different from that in rabbit in respect to its sensitivity to E-4031 and its activation threshold [1]. Since the voltage-dependent deactivation of I_K is considered to be one of the major mechanisms underlying the diastolic depolarization in SA node cells [12, 15], ionic mechanisms underlying the pacemaker potential might differ in these two species.

The first aim of the present study is to characterize the pacemaker SA node cells by recording spontaneous action potentials and whole-cell membrane current components in the guinea-pig and subsequently, to examine the presence of I_{st} in guinea-pig SA node cells. We conclude that the properties of I_{st} are almost identical in guinea pig and rabbit.

J. Guo · T. Mitsuiye · A. Noma (✉)
Department of Physiology, Faculty of Medicine,
Kyoto University, Sakyo-ku, 606-01 Kyoto, Japan

Materials and methods

Single cell preparation

Cardiac myocytes were obtained from guinea-pig SA nodes using a enzymatic dissociation technique similar to that described elsewhere [8]. Adult guinea-pigs weighing 200–300 g were anaesthetized with pentobarbitone sodium (40 mg/kg). Under artificial respiration the chest cavity was opened and the aorta was cannulated in situ to start perfusion of the coronary vessels with the control Tyrode solution. The heart was then excised and mounted on a

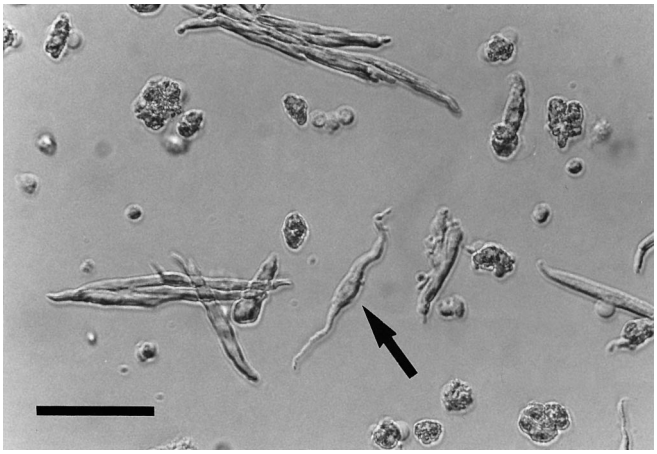

Fig. 1 Isolated myocytes from guinea-pig sino-atrial (SA) node. The fusiform cell indicated by the *arrow* is a representative cell which showed spontaneous action potentials, the nicardipine-sensitive late current NSLC and the hyperpolarization activated cation current (I_f). Other cells are considered as atrial and intermediate type. The *black bar* represents 100 μm

Langendorff-type apparatus. The perfusion solution was switched from the control Tyrode to a Ca^{2+}-free Tyrode, and then to the same solution containing 0.04% collagenase (Wako, Tokyo, Japan). After 10–15 min collagenase treatment, the SA node region bordered by the crista terminalis, atrial septum and the cranial and caudal vena cava [16] was excised and cut into small strips 0.5–1 mm wide. The strips of the SA node were further incubated in the Ca^{2+}-free Tyrode solution containing 0.1% collagenase and 0.01% elastase (Boehringer, Germany) for 10–13 min. After the enzyme treatment, myocytes were mechanically dissociated in high-K^+, low-Cl^- solution, and stored at 4°C for later experiments on the day of dissociation.

The pacemaker SA node cells of the guinea-pig (indicated by the arrow in Fig. 1) showed spontaneous contractions in a regular rhythm and faint striations, and were more spindle-like than those of the rabbit [4]. The cells were 5–10 μm wide and 50–80 μm long and the membrane capacitance of cells used in the present study was 38.6 ± 7.2 pF (mean ± SD, n = 14). The pacemaker SA node cells were very scarce. The rest of cells were quiescent or contracted irregularly, probably due to transient depolarization caused by the unphysiological and spontaneous release of Ca^{2+} from the sarcoplasmic reticulum.

Solutions

The control Tyrode solution contained (mM): NaCl 140.0, KCl 5.4, NaH_2PO_4 0.33, $MgCl_2$ 0.5, $CaCl_2$ 1.8, glucose 5.5 and *N*-(2-hydroxymethyl)piperazine-*N*′-(2-ethanesulphonic acid) (HEPES) 5.0. pH was adjusted to 7.4 with NaOH. The high-K^+, low-Cl^- solution contained (mM): KCl 30, K-glutamate 70, KH_2PO_4 10, $MgCl_2$ 1, taurine 20, glucose 10, ethyleneglycolbis(β-aminoethyl-ether)-*N*,*N*,*N*′,*N*′-tetraacetic acid (EGTA) 0.3 and HEPES 10 (pH = 7.3 with KOH). When appropriate, the concentration of Ca^{2+} in the external solution was altered without replacement. The Na^+-free solution was prepared by replacing NaCl with equimolar *N*-methyl-D-glucamine-HCl (NMDG). The Cs^+ internal solution contained (mM): CsOH 125.0, tetraethylammonium chloride (TEA-Cl) 20.0, EGTA 5.0, $CaCl_2$ 1.2, adenosine 5'-triphosphate Mg salt (ATP-Mg) 5.0, guanosine 5'-triphosphate Na_2 salt (GTP-Na_2) 0.1, adenosine 3',5'-cyclic monophosphate (cyclic AMP) 0.05 and HEPES 10.0 (pH = 7.2 with aspartic acid). The concentration of free Ca^{2+} ($[Ca^{2+}]$) in this internal solution was approximately 50 nM according to [5] and [21]. The K^+ internal solution for whole cell recordings contained (mM): K-aspartate 130, $MgCl_2$ 1, ATP-K_2 5, GTP-Na_2 0.1, EGTA 0.2, HEPES 10 (pH = 7.2 with KOH).

Whole-cell voltage-clamp experiments

The whole-cell voltage clamp method was essentially the same as that described by Hamill et al. [11]. Action potentials were measured in the current-clamp configuration. The external tip diameter of glass suction pipettes was 2–3 μm, and the electrical resistance 3–7 MΩ. Current and voltage signals from a patch clamp amplifier (EPC-7, List, Darmstadt, Germany) were sampled simultaneously by an on-line computer system (PC98, NEC, Tokyo, Japan) and stored on magnetic tape (TEAC RD-120T, TEAC, Japan). The low cut-off frequency of the current signal was set to 3 kHz.

All data presented in this paper were corrected for a liquid junction potential of –10 mV between the aspartate-rich pipette solution and the Tyrode solution. Data are given as mean ± SEM unless otherwise indicated. All experiments were carried out at 34 ± 1°C.

Results

Electrophysiological identification of the pacemaker SA node cell

To search for pacemaker cells within the dissociated SA node cells, action potentials were recorded from regularly beating myocytes. The typical pacemaker action potentials as shown in Fig. 2 were recorded from only a very limited number of SA node cells. The action potentials were characterized by slow diastolic depolarization followed by a smooth transition to the upstroke of the action potential (Fig. 2). The parameters of the spontaneous action potentials are summarized in Table 1. These parameters of action potential are very similar to those

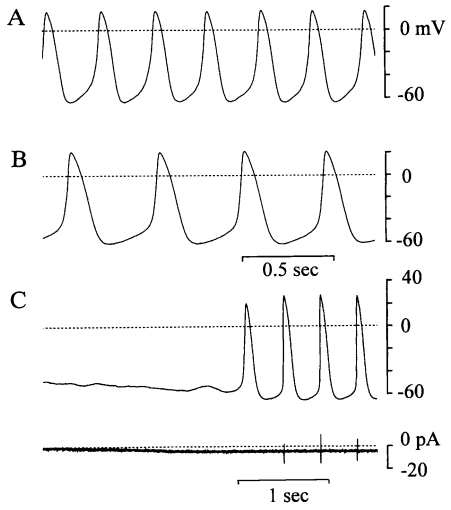

Fig. 2 A–C Spontaneous action potentials of guinea-pig SA node cells, revealed by switching from the voltage-clamp mode to the current-clamp mode (zero current), **A** and **B** represent different cells. The *dotted line* indicates zero voltage. In **C** an increasing hyperpolarizing current was injected (*lower trace*) to initiate the spontaneous action potential (*upper trace*). Note the different *time calibration* in C. The K^+-rich pipette solution was used

Table 1 Action potential parameters of single guinea-pig sino-atrial node cells[a]

parameter	mean
MDP (mV)	–58.7 ± 3.8
Overshoot (mV)	17.9 ± 4.8
Upstroke velocity (V/s)[b]	3.6 ± 1.3
AP duration (ms)	87.3 ± 24.1
Beat rate (min^{-1})	191 ± 76.6

[a] Data are mean ± SD (n=7), corrected for the liquid junction potential of –10 mV (*MDP*=maximum diastolic potential, AP=duration action potential duration measured at 50% repolarization)
[b] Upstroke velocity represents the maximum rate of rise of the action potential calculated from records sampled at 2 kHz

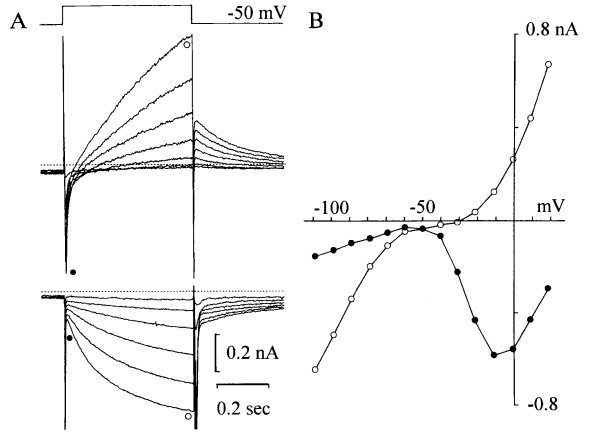

Fig. 3A, B Whole-cell membrane currents in a guinea-pig SA node cell. **A** Membrane currents induced by depolarizing (*upper panel*) and hyperpolarizing (*lower panel*) pulses are superimposed. The pulse protocol is shown at the *top*, the holding potential was –50 mV and test pulses ranged from –40 to 20 mV with an interval of 10 mV in the *upper panel*, and from –60 to –110 mV in the lower panel. **B**, Current/Voltage (*I*/*V*) relation of the peak inward current on depolarization or the initial current level on hyperpolarization (●). The late current levels (○) were measured near the end of the 500 ms pulse. The K^+-rich pipette solution was used

recorded from single rabbit SA node cells [4] and from multicellular SA node preparations from the guinea-pig [3, 16]. In most cells the spontaneous firing rate was around 200 min^{-1} (Fig. 2A, 204 min^{-1}), similar to that in multicellular guinea-pig SA node preparations (218 min^{-1} [16]).

In several experiments, the spontaneous rhythm decelerated or stopped after breaking the patch membrane to start the whole-cell recording (Fig. 2B, 130 min^{-1}). In these cells (Fig. 2C), spontaneous action potentials could be initiated by applying a slight hyperpolarizing current to compensate leak current through the tight seal at the electrode tip. The large variety in the spontaneous rate between cells in Table 1 might be partly due to variation in the leak conductance through the tight seal.

To characterize further the pacemaker cells, whole-cell membrane currents were recorded in those cells showing the spontaneous action potentials. From the holding potential of –40 or –50 mV, hyperpolarizing pulses activated a slowly increasing inward current, I_f (Fig. 3A, lower panel), and switching off test pulses activated I_{Na}, followed by the inward tail current due to deactivation of the I_f channel. The activation threshold of I_f was about –70 mV in all 15 pacemaker SA node cells. In contrast, no obvious I_f was observed in most quiescent cells, except in a small number of intermediate cells, which showed a small I_f on hyperpolarization beyond –90 mV. These cells showed atrial-type action potentials when stimulated by brief current pulses.

Depolarizing pulses from a holding potential of –50 mV induced a transient inward current followed by a slow increase in the outward current (Fig. 3A, upper panel). The peak current/voltage (*I*/*V*) relation for the transient inward current (Fig. 3B) showed an activation threshold of about –40 mV and a current magnitude reached a maximum around –10 mV. Since the current was blocked by 1 μM nicardipine, the transient inward current was attributed to the L-type Ca^{2+} channel.

The time-dependent outward current during depolarization and the tail current on repolarization were hardly affected by E-4031 (n = 5, data not shown) as reported previously by Anumonwo et al. [1]. These authors therefore attributed the current to I_{Ks}. Consistent with I_{Ks} [18], the activation threshold of the outward current was around –30 mV and no obvious inward rectification was observed in the voltage range examined (up to 20 mV in the cell shown in Fig. 3 and 50 mV in the other five cells).

No clear transient outward current was observed in the pacemaker SA node cells. The inward rectifier K^+ ($I_{K,1}$) channels were apparently also absent in these cells, since the initial current levels with various hyperpolarizing pulses were hardly affected by applying the K^+-free solution (n = 3). We failed to demonstrate the low-threshold Ca^{2+} channels ($I_{Ca,T}$) in experiments using both the Na^+-free solution and a holding potential of –80 mV, probably due to a limited number of successful experiments (n = 5).

Sustained inward current

To this point we had characterized the pacemaker cells in the guinea-pig SA node by recording action potentials and membrane currents. We then addressed the question of whether I_{st} is present in these pacemaker cells. Membrane K^+ conductance was blocked by using the Cs^+-rich internal solution and inward current components were examined for the major characteristics of I_{st}. Since the activation threshold of I_{st} has been reported to be around –70 mV [8], the holding potential was set to –80 mV after blocking I_f by adding 5 mM Cs^+ to the control Tyrode solution. The activation of I_{Na} at the onset of the depolarizing pulse was ignored in this study because of plausible clamp failure. In Fig. 4A, membrane currents recorded before and after applying nicardipine are superimposed to demonstrate the nicardipine-sensitive current components, and the isochronal *I*/*V* relations measured near the

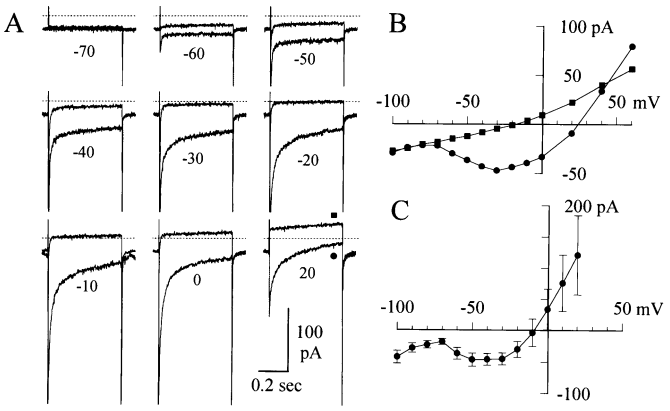

Fig. 4 A–C Nicardipine-sensitive current components in a pacemaker SA node cell. **A** Current traces in control (●) and after applying 1 μM nicardipine (■) are superimposed for the potential indicated (magnitude in millivolts). The currents were elicited by various depolarizing pulses of 0.5 s from the holding potential of –80 mV. The peaks of the Na^+ current (I_{Na}) and/or the current through L-type Ca^{2+} channels ($I_{Ca,L}$) are out of scale at –50 to 0 mV. *Dotted lines* indicate the zero current level. **B** The isochronal *I*/*V* relation measured near the end of the pulses in the experiment shown in **A**; ●, control; ■, in 1 μM nicardipine. **C** The average of the isochronal *I*/*V* relation measured near the end of the test pulse in nine cells. The *vertical bars* indicate SEM. The Cs^+-rich pipette solution was used. The cell membrane capacitance was 46 pF

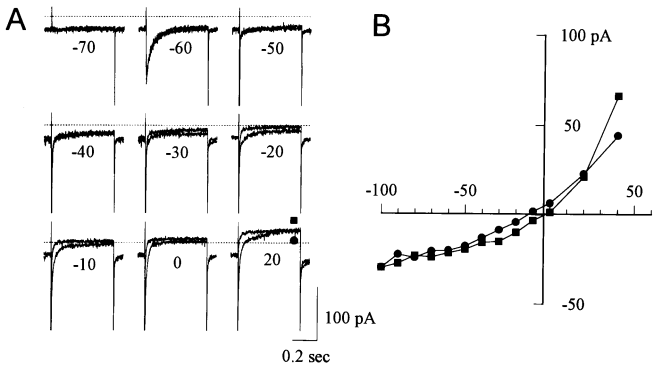

Fig. 5A, B Nicardipine-sensitive current components in a rod-shaped SA node cell. The same explanation as in Fig. 3 is applicable to **A** and **B**. The cell membrane capacitance was 52 pF

end of the pulse are demonstrated in Fig. 4B. The time-dependent decrease of the difference current during pulses positive to –40 mV might be explained largely by the time-dependent inactivation of $I_{Ca,L}$. However, the inactivation of $I_{Ca,L}$ is usually more extensive, and we cannot expect a large sustained $I_{Ca,L}$ component near the end of a 500 ms-pulse (see Fig. 5). Furthermore, the inward currents at –60 and –50 mV are difficult to explain with $I_{Ca,L}$, which is usually activated at potentials positive to –40 mV. In fact, the sustained current component was the first indication of the presence of a novel current system, I_{st}, in the rabbit SA node cell. Here, the nicardipine-sensitive current component measured near the end of the pulse (late current) is abbreviated as NSLC.

The late *I*/*V* relations in eight experiments are averaged in Fig. 3C. If we assume a linear background conductance by extrapolating the conductance from potentials more negative than –70 mV, the magnitude of the NSLC at –50 mV was 46.5 ± 10.5 pA (n = 9). The apparent reversal potential of NSLC may be determined by both the inward Na^+ current through the I_{st} channels and the outward Cs^+ current through the $I_{Ca,L}$ channel.

Alternatively, NSLC may be totally through $I_{Ca,L}$ channel provided that the voltage- and time-dependent gating of the $I_{Ca,L}$ channel in the SA node cell is different to that in other cell types. This possibility is unlikely in the rabbit SA node. For example, the rabbit $I_{Ca,L}$, which was isolated by depleting the extracellular $[Na^+]$ ($[Na^+]_o$), shows an activation threshold around –40 mV and the amplitude of the $I_{Ca,L}$ window component is quite small [9, 10]. Because these findings are critical if a new current system is to be proposed, we examined $I_{Ca,L}$ in transitional guinea-pig SA node cells showing no obvious I_f and having the appearance of the rod cells in Fig. 1 (Fig. 5). It is evident that the activation threshold of $I_{Ca,L}$ was indeed about –30 mV and the sustained window component was negligibly small near the end of the pulse (the maximal amplitude of the NSLC was 8.0 ± 0.7, n = 6, at –20 mV, 500 ms), confirming that the guinea-pig SA node $I_{Ca,L}$ channel has similar gating properties as in other cell types. The transient inward current at –60 mV in Fig. 5 was resistant to nicardipine and probably due to activation of the Na^+ channel.

Ion selectivity of NSLC and $I_{Ca,L}$

In the rabbit SA node Na^+ has been suggested to carry I_{st} in contrast to $I_{Ca,L}$ which is carried by Ca^{2+} [9]. To test this possibility, effects of decreasing external Ca^{2+} on the NSLC were examined. Both I_{Na} and probably $I_{Ca,T}$ were inactivated by a conditioning pulse to –40 mV from the holding potential of -80 mV. In the control 1.8 mM $[Ca^{2+}]_o$ solution, activation of NSLC at –60 and –50 mV and $I_{Ca,L}$ at more positive potentials were evident (Fig. 6A, left column). In the isochronal *I*/*V* relation at about 0.5 s (the solid circles in Fig. 6B), the activation of NSLC was observed at potentials less negative than –70 mV. Decreasing $[Ca^{2+}]_o$ to 0.1 mM largely removed the transient inward current $I_{Ca,L}$ but NSLC remained clear at –60, –50, –40 and –20 mV in the current recordings (Fig. 6A) and in the *I*/*V* curve (solid triangles in Fig. 6B). Essentially the same results were obtained in all five cells.

Superfusion with Na^+-free solution frequently reduced $I_{Ca,L}$, most probably due to a transient overload of the intracellular $[Ca^{2+}]$ ($[Ca^{2+}]_i$) through the reverse mode of the Na/Ca exchange. To detect and discard this artifactual modulation, both NSLC and $I_{Ca,L}$ were recorded every 10 s using a compound test pulse as shown in Fig. 7 (inset). The first depolarizing pulse from –80 to –50 mV activated both NSLC and I_{Na}, while the second depolarizing pulse to –10 mV following the conditioning pulse to –40 mV activated $I_{Ca,L}$, probably in addition to a

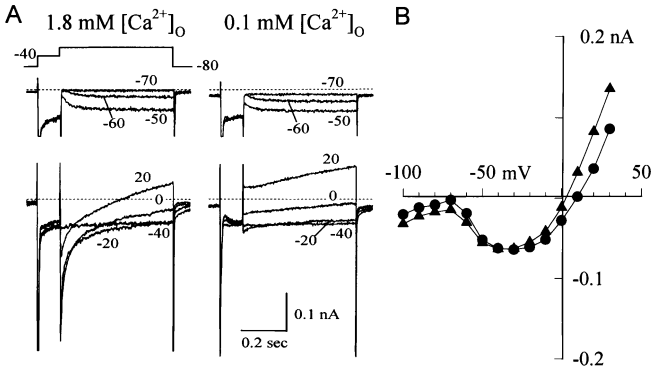

Fig. 6A, B Effect of decreasing extracellular $[Ca^{2+}]$($[Ca^{2+}]_o$) on NSLC and $I_{Ca,L}$. **A** Current traces are superimposed in 1.8 mM $[Ca^{2+}]_o$ control solution (*left column*) and in 0.1 mM $[Ca^{2+}]_o$ (*right column*). NSLC and $I_{Ca,L}$ were separated from I_{Na} by inactivating I_{Na} using a conditioning pulse to –40 mV for 100 ms before the test pulse as indicated at the *top*. The peaks of I_{Na} at the onset of conditioning pulses are out of scale. **B** *I*/*V* relations of the late currents measured near the end of the test pulses in 1.8 (●) and 0.1 mM (▲) $[Ca^{2+}]_o$ solutions in the experiment shown in **A**. The Cs^+-rich pipette solution was used

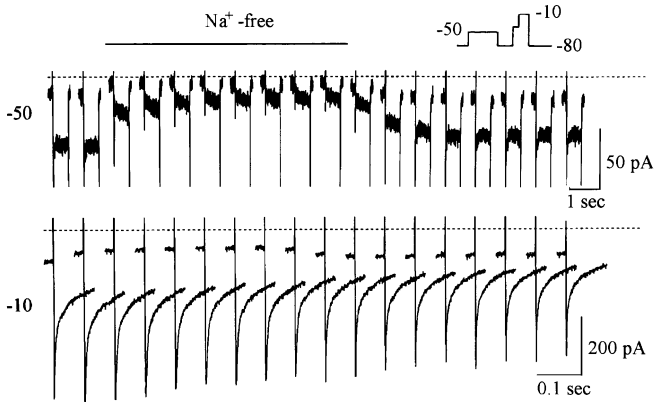

Fig. 7 Effects of omitting external Na^+ on NSLC and $I_{Ca,L}$. The compound test pulse in the *inset* was used to record NSLC with the first pulse to –50 mV and $I_{Ca,L}$ with the second test pulse to –10 mV following a conditioning pulse of –40 mV. The current traces recorded every 10 s are illustrated according to the time sequence before, during and after the perfusion of Na^+-free *N*-methyl-D-glucamine (NMDG) solution as indicated at the *top*. Note the different *time* and *current scales* between the *upper* and *lower rows*. The holding potential was –80 mV. The Cs^+-rich pipette solution was used

relatively small I_{st}. Switching the bath solution from control Tyrode solution to the Na^+-free NMDG solution largely depressed NSLC at –50 mV, while the amplitude of $I_{Ca,L}$ at –10 mV was not much changed. The continuous and gradual decrease of $I_{Ca,L}$ amplitude might be due to a spontaneous run-down of the channel (Fig. 7). The decrease of NSLC was almost completely reversed by changing the bath solution back to the control. In five cells NSLC at –50 mV was decreased from –49.1 ± 2.2 to –10.9 ± 2.0 pA (21.2 ± 3.9%) within 1–2 min perfusion with the NMDG solution. The small NSLC remaining in the NMDG solution might be due to incomplete removal of Na^+ around the cell in the limited perfusion time. It is suggested that NSLC is carried mainly by Na^+ under physiological conditions.

Pharmacological properties of the NSLC

In the following experiments, NSLC was isolated by suppressing $I_{Ca,L}$ in the 0.1 mM $[Ca^{2+}]_o$ solution and *I*/*V* relations for NSLC measured directly from the descending limb of ramp pulses (Fig. 8B, inset). Although NSLC is sensitive to $[Na^+]_o$, the pharmacological properties of the NSLC were different from those of Na^+ channels.

Figure 8 shows effects of the dihydropyridine antagonist nicardipine and the agonist Bay K 8644 on the NSLC. Like $I_{Ca,L}$, the NSLC was greatly increased by 1 μM Bay-K 8644. The increase was more prominent at negative potentials than at positive potentials and the activation threshold of NSLC was slightly shifted to more negative potentials in the *I*/*V* curve in Fig. 8B. Consecutive application of 1 μM nicardipine completely blocked the NSLC and resulted in an almost linear *I*/*V* relation. The three *I*/*V* curves – control, 1 μM Bay K and 1 μM nicardipine – intersected at almost the same point. The apparent reversal potential of about 28 mV in Fig. 8 is in

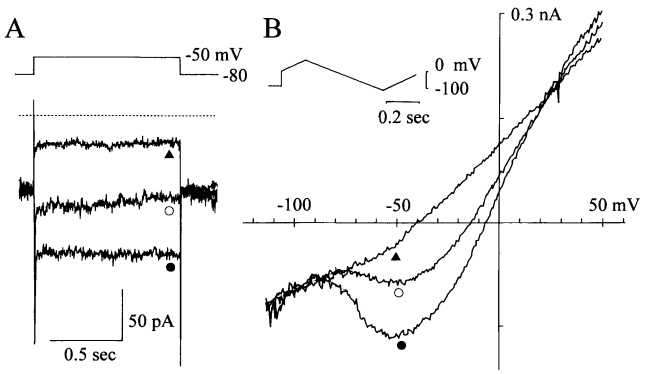

Fig. 8A, B Effects of Bay K 8644 and nicardipine on NSLC. **A** NSLC induced by depolarization to –50 mV from –80 mV in the control (○), 1 μM Bay K 8644 (●) and 1 μM nicardipine (▲) are superimposed. **B** *I*/*V* relations measured from the descending limb of the ramp pulse (–0.32 V/s) are superimposed under the conditions indicated by the *symbols*. The square pulse and ramp command were given alternately at 10-s intervals. The Cs^+-rich pipette solution was used

good agreement with that of the nicardipine-sensitive current in rabbit [8, 9]. Bay K 8644 (1 μM) increased NSLC to 192 ± 14% of control at the peak potential of –50 to –40 mV (n = 7).

Characteristics of the NSLC similar to those of the $I_{Ca,L}$ channel were also obtained in respect of the autonomic regulation of NSLC. As shown in Fig. 9, 0.1 μM isoprenaline increased NSLC nearly twofold. This increase was completely reversed by adding 5 μM acetylcholine (ACh) in the presence of 0.1 μM isoprenaline. In six experiments, NSLC was increased to 154.5 ± 7.3% of control by 0.1 μM isoprenaline and adding 5 μM ACh in the presence of isoprenaline reduced NSLC to 88.1 ± 8.6% of control. Applying 5 μM ACh alone

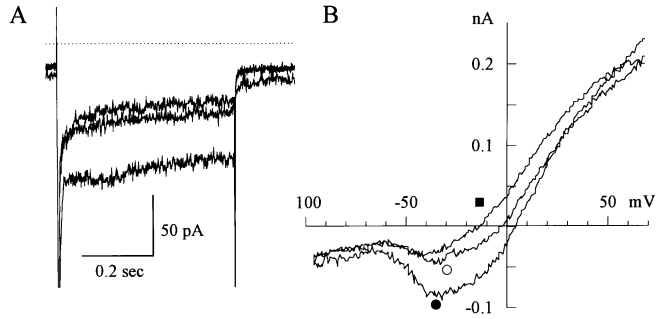

Fig. 9A, B Effects of isoprenaline and acetylcholine (ACh) on NSLC. **A** NSLC induced by depolarization to –50 mV from –80 mV in the control (○), 0.1 μM isoprenaline (●) and 5 μM ACh in the presence of isoprenaline (■) are superimposed. **B** The *I*/*V* relations obtained under the corresponding conditions. The Cs^+-rich pipette solution was used

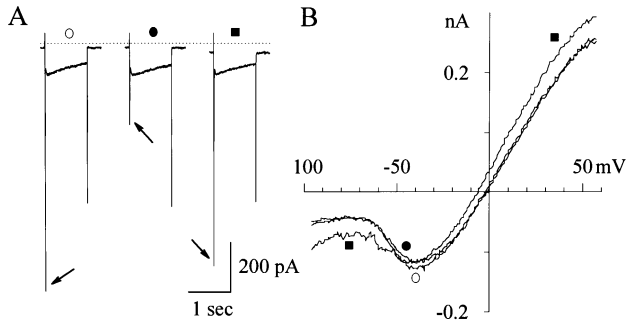

Fig. 10A, B Effects of tetrodotoxin (TTX) on NSLC and I_{Na}. **A** Current recordings were induced by a 1-s depolarizing pulse to –50 mV from the holding potential of –80 mV, before (○), during (●), and after (■) washing off TTX. The *arrow* indicates the peak of the transient inward current at the onset of the pulse. **B** The *I*/*V* relations obtained under the corresponding conditions. The Cs^+-rich pipette solution was used

slightly inhibited NSLC in only two out of seven cells (12% and 15% inhibition).

The window current of I_{Na} [2] might be included in the Na^+-sensitive NSLC. To test this possibility both I_{Na} and NSLC were recorded by a depolarizing pulse to –50 mV from –80 mV during the application of 30 μM tetrodotoxin (TTX). It is evident by comparing the TTX record (Fig. 10A, solid circles) with both the control (open circles) and wash-out records (solid squares) that TTX largely blocked the transient inward current at the onset of depolarization, leaving NSLC almost constant. When *I*/*V* curves were obtained with ramp pulses in the same cell (Fig. 10B), the TTX-insensitive nature of NSLC was obvious (n = 5). It is concluded that the window component of I_{Na} is negligibly small in the guinea-pig SA node.

Discussion

The present voltage clamp experiment in guinea-pig pacemaker cells demonstrate the existence of the sustained inward current NSLC which showed essentially the same characteristics as the I_{st} described for the rabbit SA node cell [8, 9]. We conclude that NSLC in the present study in the guinea-pig is largely due to I_{st} channels in addition to a minor component of the $I_{Ca,L}$ window. Since the amplitude of NSLC is much smaller in quiescent SA node cells in both rabbit and guinea-pig, it is suggested that the expression of a gene encoding the I_{st} channel in addition to the I_f channel may determine the pacemaker cells in the developing heart in a variety of mammalian species.

In both rabbit and guinea-pig hearts, $I_{Ca,L}$ was activated at potentials less negative than –40 mV in the quiescent cells dissociated from the SA node region ([8, 10] for review [13]). In these cells, depolarization to –60 and –50 mV induced no nicardipine-sensitive inward current, indicating the absence of I_{st}. $I_{Ca,L}$ isolated by reducing $[Na^+]_o$ in the pacemaker cells [9, 10] also showed an activation threshold at about –40 mV. We therefore consider that the characteristics of the L-type Ca^{2+} channels are common between the non-pacemaker [13] and pacemaker cells. In contrast, the threshold for I_{st} was around –60 to –70 mV in both the rabbit [8] and guinea-pig SA nodes, and little inactivation was observed at –60 to –50 mV. I_{st} was not affected by decreasing $[Ca^{2+}]_o$, but was strongly inhibited by reducing $[Na^+]_o$. The new characteristics of I_{st} determined in this study were, firstly, that I_{st} is increased by Bay K 8644, a dihydropyridine agonist, and blocked by nicardipine, a dihydropyridine antagonist. This finding supports our hypothesis that the ionic channels responsible for I_{st} might have a very similar structure to the L-type Ca^{2+} channels. Secondly, ACh reversed the increase of I_{st} induced by the prior application of isoprenaline. It is suggested that the autonomic regulation of I_{st} is dependent on the same signal transduction as that of $I_{Ca,L}$; namely the channel activity is modulated by the cyclic AMP-dependent protein kinase and the activation of the adenylate cyclase through the β-adrenergic receptor-guanine nucleotide-binding protein (G protein) is antagonized by the muscarinic receptor-G protein complex [13]. In several cells ACh slightly reduced I_{st} without prior β-adrenergic stimulation. We assume that this might have been due to a high cyclic AMP level in these SA node cells, as previously suggested for the regulation of $I_{Ca,L}$ in rabbit SA node myocytes [17]. In preliminary experiments, we could observe essentially the same effects of Bay K 8644, isoprenaline and ACh on I_{st} in rabbit SA node cells (unpublished observations).

Theoretically the depolarization-dependent activation of an inward current system, I_{st}, over the range of the the diastolic potential (–60 to –40 mV) should be favorable for diastolic pacemaker depolarization. The activation threshold of $I_{Ca,L}$ (–40 mV) is less negative than the maximum diastolic potential of around –60 mV. On the other hand, $I_{Ca,L}$ is responsible for the rapid upstroke of the spontaneous action potential. We hypothesize that the sequential activation of I_{st} followed by $I_{Ca,L}$ underlies the smooth transition from the slow diastolic depolarization to the rapid upstroke of the action potential. The positive

chronotropic effect of stimulating the β-adrenergic receptor may be mediated mainly by an increase in I_{st}.

The parameters of the spontaneous action potential in guinea-pig single SA node cells were essentially the same as those examined in multicellular preparations [3, 16, 20] and also in single rabbit SA node cells [14]. Interestingly, both the amplitude of I_{st} and the cellular membrane capacitance were quite similar in rabbit (49 pA and 47 pF, [8]) and guinea-pig (46 pA and 38 pF, present study). It seems that $I_{Ca,L}$, I_{st} and I_f in guinea-pig SA node cells are essentially the same as those in the rabbit. Neither the inward rectifier K^+ current nor the transient outward current was found. The composition of the guinea-pig delayed rectifier K^+ current alone seems differ from that in the rabbit SA node. In the latter case the outward tail current (I_{Kr}) on repolarization is almost completely blocked by E-4031 [15, 22], while in the guinea-pig SA node cells the outward tail current is hardly affected by E-4031 [1]. Irrespective of the difference in the drug sensitivity, the time-dependent slow deactivation of the delayed K^+ current on repolarization may be responsible for the slow diastolic depolarization [19]. The activation threshold of I_f is more negative than –70 mV (in the present study, see also [6, 7]) thus, it is difficult to assume a large contribution of I_f to diastolic depolarization.

Acknowledgements The authors thank Dr. M. Takano for his discussion during the work, Mr. Fukao for his technical assistance and Kanako Fujita for her secretarial services. The work was supported by a research grant from the Ministry of Education, Science and Culture of Japan.

References

1. Anumonwo JMB, Freeman LC, Kwok WM, Kass RS (1992) Delayed rectification in single cells isolated from guinea pig sinoatrial node. Am J Physiol 262:H921–H925
2. Baruscotti M, DiFrancesco D, Robinson RB (1996) A TTX-sensitive inward sodium current contributes to spontaneous activity in newborn rabbit sino-atrial node cells. J Physiol (Lond) 492:21–30
3. Campbell GD, Edwards FR, Hirst GDS, O'Shea JE (1989) Effects of vagal stimulation and applied acetylcholine on pacemaker potentials in the guinea-pig heart. J Physiol (Lond) 415: 57–68
4. Denyer JC, Brown HF (1990) Rabbit sino-atrial node cells: isolation and electrophysiological properties. J Physiol (Lond) 428:405–424
5. Fabiato A, Fabiato F (1979) Calculator programs for computing the composition of the solutions containing multiple metals and legends used for experiments in skinned muscle cells. J Physiol (Paris) 75:463–505
6. Frace AM, Maruoka F, Noma A (1992) External K^+ increases Na^+ conductance of the hyperpolarization-activated current in rabbit cardiac pacemaker cells. Pflügers Arch 421:97–99
7. Ginneken ACG van, Giles WR (1991) Voltage clamp measurements of the hyperpolarization-activated inward current I_f in single cells from rabbit sino-atrial node. J Physiol (Lond) 434: 57–83
8. Guo J, Ono K, Noma A (1995) A sustained inward current activated at the diastolic potential range in rabbit sino-atrial node cells. J Physiol (Lond) 483:1–14
9. Guo J, Ono K, Noma A (1996) Monovalent cation conductance of sustained inward current in rabbit sinoatrial node cells. Pflügers Arch (in press)
10. Hagiwara N, Irisawa H, Kameyama M (1988) Contribution of two types of calcium currents to the pacemaker potentials of rabbit sino-atrial node cells. J Physiol (Lond) 395:233–253
11. Hamill OP, Marty A, Neher E, Sakmann B, Sigworth FJ (1981) Improved patch-clamp techniques for high-resolution current recording from cells and cell-free membrane patches. Pflügers Arch 391:85–100
12. Irisawa H, Brown HF, Giles W (1993) Cardiac pacemaking in the sino-atrial node. Physiol Rev 73:197–227
13. McDonald TF, Pelzer S, Trautwein W, Pelzer DJ (1994) Regulation and modulation of calcium channels in cardiac, skeletal, and smooth muscle cells. Physiol Rev 74:365–507
14. Nakayama T, Kurachi Y, Noma A, Irisawa H (1984) Action potential and membrane currents of single pacemaker cells of the rabbit heart. Pflügers Arch 402:248–257
15. Ono K, Ito H (1995) Role of rapidly activating delayed rectifier K^+ current in sinoatrial node pacemaker activity. Am J Physiol 269:H453–H462
16. Opthof T, De Jonge B, Mackaay AJC, Bleeker WK, Masson-Pevet M, Jongsma HJ, Bouman LN (1985) Functional and morphological organization of the guinea-pig sinoatrial node compared with the rabbit sinoatrial node. J Mol Cell Cardiol 17:549–564
17. Petit-Jacques J, Bois P, Bescond J, Lenfant J (1993) Mechanism of muscarinic control of the high-threshold calcium current in rabbit sino-atrial node myocytes. Pflügers Archiv 423: 21–27
18. Sanguinetti MC, Jurkiewicz NK (1990) Two components of cardiac delayed rectifier K^+ current: differential sensitivity to block by class III antiarrhythmic agents. J Gen Physiol. 96: 195–215
19. Shibasaki T (1987) Conductance and kinetics of delayed rectifier potassium channels in nodal cells of the rabbit heart. J Physiol (Lond) 387:227–250
20. Sohn HG, Vassalle M (1995) Cesium effects on dual pacemaker mechanisms in guinea pig sinoatrial node. J Mol Cell Cardiol 27:563–577
21. Tsien RY, Rink TJ (1980) Neutral carrier ion-selective microelectrodes for measurement of intracellular free calcium. Biochim Biophys Acta 599: 623–638
22. Verheijck EE, Ginneken ACG van, Bourier J, Bouman LN (1995) Effects of delayed rectifier current blockade by E-4031 on impulse generation in single sinoatrial nodal myocytes of the rabbit. Circ Res 76:607–615